

## Magnetization and electron-spin-resonance studies of doped NbSe<sub>3</sub>

M. C. Aronson\* and M. B. Salamon

*Department of Physics, University of Illinois at Urbana-Champaign, 1110 West Green Street, Urbana, Illinois 61801  
and Materials Research Laboratory, University of Illinois at Urbana-Champaign, 104 South Goodwin Avenue,  
Urbana, Illinois 61801*

(Received 16 February 1988)

We have performed dc-magnetization and electron-spin-resonance (ESR) measurements on undoped, Ta-doped, and V-doped NbSe<sub>3</sub>, at temperatures ranging from 1.7 to 200 K. The magnetization measurements show that although Ta impurities are nonmagnetic, V impurities are weakly magnetic. In the undoped and Ta-doped samples, the resonance involves unpaired conduction electrons; the ESR spin susceptibility,  $g$  factor, and linewidth exhibit maxima near the lower charge-density-wave (CDW) transition. We suggest that this is the result of changes in the non-CDW band structure with induced gap formation. The resonance in the V-doped sample is quite different, mixing the properties of conduction-electron and local-moment resonances.

### I. INTRODUCTION

NbSe<sub>3</sub> undergoes two independent charge-density-wave (CDW) transitions at  $T_{p1}=145$  K and  $T_{p2}=60$  K.<sup>1</sup> As a result of these transitions, gaps form at the Fermi surface, significantly altering the electronic properties. Since NbSe<sub>3</sub> is metallic at the lowest temperatures, some unpaired conduction electrons remain after CDW formation. These electrons dominate such measured quantities as the electric resistance,<sup>1</sup> magnetic susceptibility,<sup>2</sup> and specific heat<sup>3</sup> at low temperature. However, interpreting these experimental results near the CDW transitions is complicated by the difficulties involved with separating the contributions from the CDW and non-CDW bands. We will demonstrate in this paper that electron-spin resonance (ESR) is particularly well suited for studying the effects of CDW formation of the non-CDW bands since only the non-CDW electrons participate in the resonance, and because the resonance may be observed at temperatures well above both CDW transitions.

In conjunction with the ESR experiment, we present the results of dc-magnetization experiments on undoped, Ta-doped, and V-doped NbSe<sub>3</sub> samples. These measurements show not only that NbSe<sub>3</sub> supports magnetic and nonmagnetic impurities, but also that the magnetic impurities interact strongly with the conduction electrons. We have performed ESR measurements on the same samples at temperatures ranging from  $\sim 10$  to 200 K. In both the undoped and Ta-doped samples, the observed resonance involves non-CDW electrons; the resonance parameters are sensitive to variations in the band structure caused by CDW formation. We propose a scenario for the development of induced gaps on the non-CDW band, and show how this gap formation is reflected in the electronic properties. The resonance in the V-doped sample mixes the properties of conduction-electron and local-moment resonances.

### II. MAGNETIZATION OF DOPED NbSe<sub>3</sub>

Undoped as well as V- and Ta-doped samples of NbSe<sub>3</sub> were prepared by the vapor transport method from stoichiometric quantities of Nb, Se, V, and Ta. Powder x-ray scans were performed on the resulting crystals to verify the correct crystal structure and to check for the inclusion of contaminant phases. Energy-dispersive x-ray analysis (EDS) was performed on representative crystals from each batch to determine the average doping level and the range of levels within a single batch. This technique, sensitive to  $\sim 500$  ppm in relative V concentration and with an absolute sensitivity of  $\sim 500$  ppm, found that dopant levels can vary by a factor of 2–3 among crystals from a single batch.

The magnetization measurements were performed with a Biotechnology, Inc. (S.H.E.) superconducting-quantum-interference-device-based magnetometer with a sensitivity  $\sim 10^{-8}$  emu. Approximately 10 mg of crystals were loosely packed into a thin wall Suprasil quartz capsule. The magnetization was measured in a 40-kOe field at temperatures ranging from 1.7 to 200 K; the small value of the susceptibility of NbSe<sub>3</sub> precluded any study of the field dependence of the magnetization. We assume that the magnetization is the product of the sample susceptibility and the applied field and that demagnetizing factors are negligible. The data were corrected for the core diamagnetism of  $-13 \times 10^{-5}$  cm<sup>3</sup>/mol, which was estimated using Pascal's constants. The results of these measurements for undoped, Ta-doped, and several V-doped samples are graphed in Fig. 1.

The Ta-doped and undoped samples have a susceptibility which increases with increasing temperature, as previously reported.<sup>2</sup> In these samples, the temperature dependence of the susceptibility well below the CDW transitions is that expected for a Pauli susceptibility in the presence of the CDW gaps. In contrast, the suscepti-

bility of the V-doped samples decreases with increasing temperature, suggesting the presence of local moments. The susceptibility can be adequately described with a Curie-Weiss law

$$\chi(T) = \frac{C}{T + \Theta} = \frac{1}{T + \Theta} \left[ \frac{n \mu_B^2}{k_B} \right] g(L, S, J) \sqrt{J(J+1)}, \quad (1)$$

where  $\mu_B$  is the Bohr magneton,  $k_B$  the Boltzmann constant,  $n$  the impurity concentration, and  $g$  the Landé  $g$ -factor. The V impurities are assumed to substitute for the isoelectronic Nb ions and may exist in either the  $V^{2+}$  or  $V^{3+}$  states,<sup>4</sup> suggesting values for  $g(L, S, J) \sqrt{J(J+1)}$  of 2.8 for  $V^{3+}$  and 3.8 for  $V^{2+}$ .<sup>5</sup> The corresponding range of V concentrations are compared to the microanalytic results in Table I; it is striking to note that the V

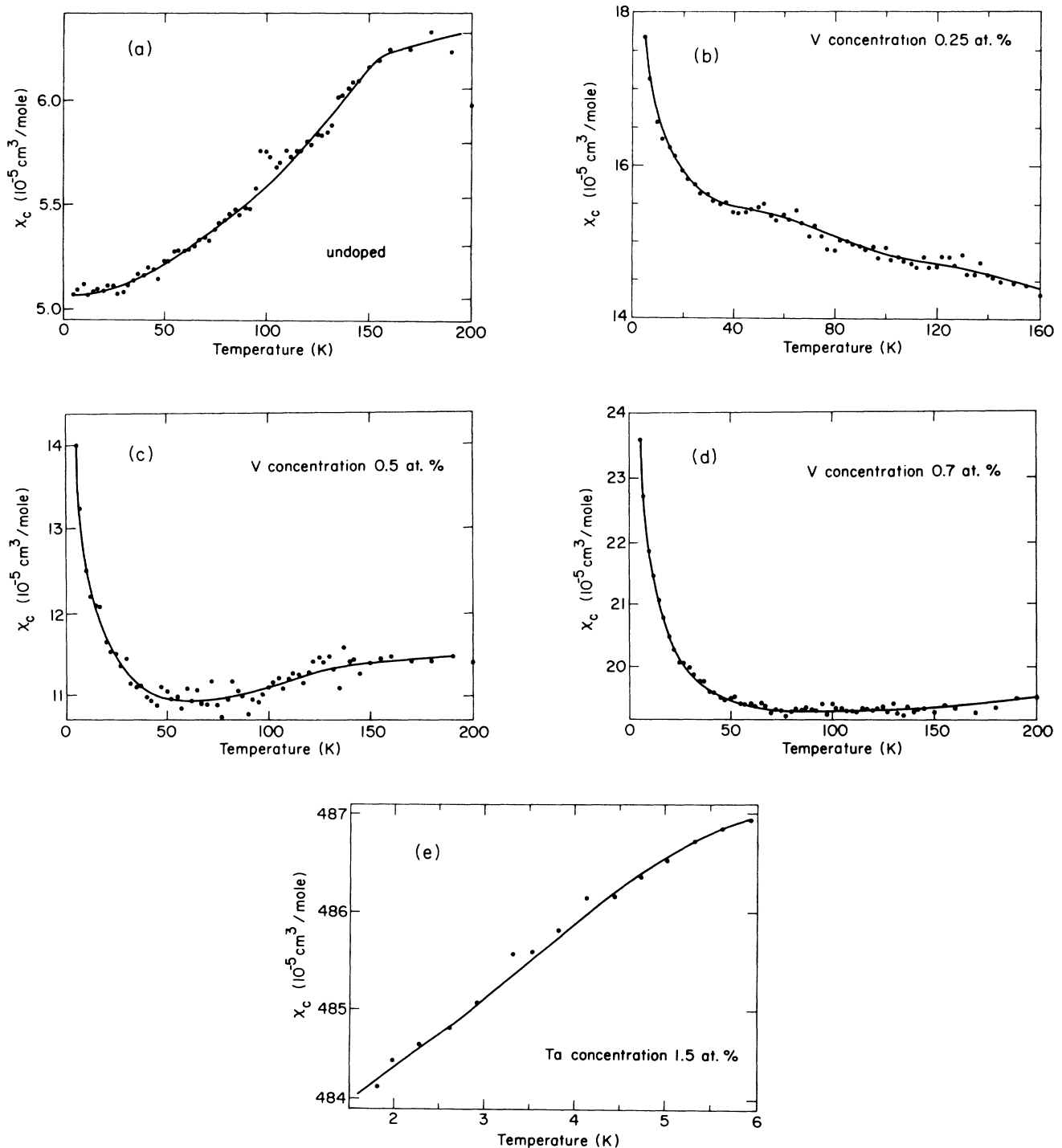


FIG. 1. Temperature dependence of the magnetic susceptibility in (a) undoped (b)  $\sim 0.25$  at. % V-doped (c)  $\sim 0.5$  at. % V-doped (d)  $\sim 0.7$  at. % V-doped, and (e)  $\sim 1.5$  at. % Ta-doped  $NbSe_3$ . Impurity levels are batch averages determined by energy-dispersive x-ray analysis (EDS).

TABLE I. Comparison of V levels in parts per million found from the Curie constant and energy-dispersive x-ray analysis (EDS).  $3k_B T\chi/\mu_B^2$  accurate to  $\sim 30$  ppm; the range of values results from uncertainty in the V moment-angular-momentum state. EDS is accurate to  $\sim 500$  ppm in relative concentration,  $\sim 5000$  ppm in absolute concentration. The range of EDS values reflects intrinsic spread in V levels among crystals from a single preparation tube.

	$\frac{3k_B T\chi}{\mu_B^2}$	EDS
Tube 1	68–125	2000–4000
Tube 2	150–275	2200–7700
Tube 5	232–426	3500–9500

concentrations obtained from the Curie constant are factors of 20–40 lower than the batch average obtained directly from the EDS measurements.

This discrepancy can be resolved in several ways. The first possibility is that the ions have their moment quenched by their interaction with the conduction electrons. Alternatively, the V ions might tend to cluster antiferromagnetically, with the observed moments primarily due to single ions outside the clusters. Since the crystals were grown by vapor transport, the V atoms are expected to enter the crystal as isoelectronic substitutions for Nb, arguing against this possibility. In lieu of firm experimental evidence for clustering, we attribute the loss of magnetic moment of V ions in NbSe<sub>3</sub> to an interaction between the V moments and the conduction electrons. In the language of the Anderson model for moment formation, the V-based *d* orbital lies very near the Fermi level, leading to appreciable mixing of the exchange split spin-up and spin-down states.

In summary, the magnetization experiments indicate the absence of localized magnetic moments in undoped and Ta-doped NbSe<sub>3</sub>. However, V is a magnetic impurity in NbSe<sub>3</sub>, with a significantly suppressed moment.

### III. ESR IN DOPED NbSe<sub>3</sub>

The ESR measurements reported here were performed on a Bruker ER300D spectrometer for temperatures ranging from 4.2 to 200 K. The samples consisted of disordered clumps of NbSe<sub>3</sub> crystals dispersed in Suprasil quartz powder. The amount of sample in the tube was typically  $\sim 100$   $\mu$ g, limited by the loss of sensitivity due to *Q* degradation caused by the presence of a metallic sample in the microwave cavity.

An example of a typical ESR derivative spectrum for undoped NbSe<sub>3</sub> is shown in Fig. 2. The spectra for samples doped with  $\sim 1$  at. % Ta and  $\sim 0.4$  at. % V are qualitatively similar. There are two main features of the spectrum: a relatively narrow resonance centered at  $\sim 3000$  Oe and a much broader resonance at lower field. While the low-field resonance is only observed when NbSe<sub>3</sub> is added to the sample tube, the high-field resonance is the result of magnetic impurities in the sample tube or quartz powder. The position of this resonance may be used as a field marker, and its integrated intensity as a means of

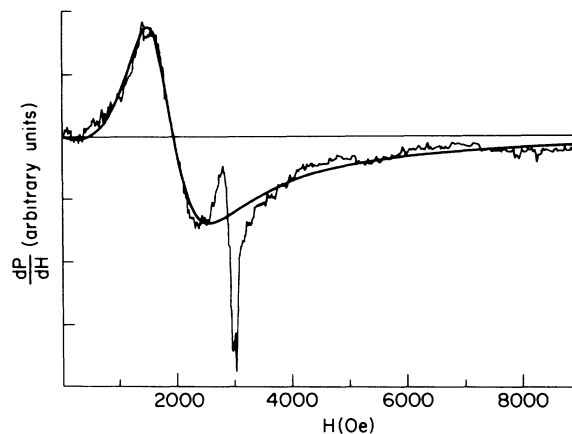


FIG. 2. ESR spectrum of undoped NbSe<sub>3</sub> at 40 K.

calibrating the sample temperature between runs. After obtaining this information, the impurity resonance and a linear background are subtracted from the measured spectrum. A nonlinear least-squares-fitting routine was used to fit the experimental spectrum to a Dysonian line shape.<sup>6,7</sup> In every case, at least 400 data points were used in the fit. The temperature dependence of the integrated ESR intensity [proportional to the static susceptibility  $\chi_{\text{ESR}}(0)$  of the resonant moments], the Landé *g* factor (extracted from the resonance field), and the linewidth are plotted in Figs. 3, 4, and 5. We will use these data to address several basic questions: first, what moments are responsible for the resonance; second, what effect do doping and temperature have on the population and moment of the resonant species, and third, what is the nature of the spin relaxation in NbSe<sub>3</sub>?

The temperature dependence of the static susceptibility  $\chi_{\text{ESR}}(0)$ , arbitrarily normalized for clarity in graphing, is plotted in Fig. 3 for undoped, Ta-doped, and V-doped samples. In the undoped and Ta-doped samples  $\chi_{\text{ESR}}(0)$

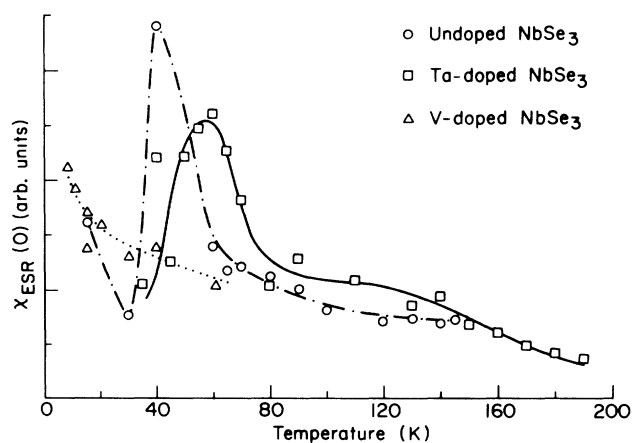


FIG. 3. Temperature dependence of the static spin susceptibility  $\chi_{\text{ESR}}(0)$ , derived from the integrated area under the ESR line, in arbitrary units. Data for undoped sample plotted as circles, Ta-doped as squares, and V-doped as triangles. Lines are guides for the eye.

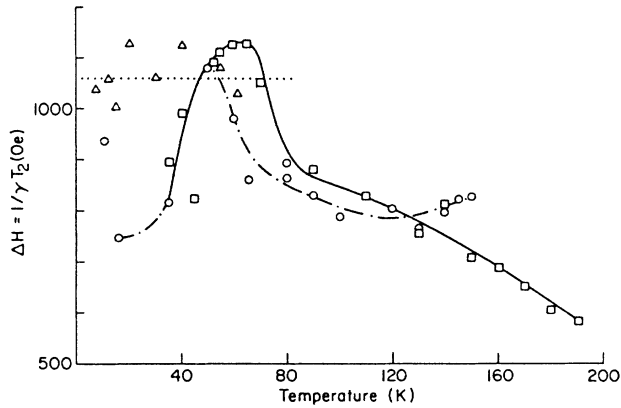


FIG. 4. Temperature dependence of the Landé  $g$  factor  $g = \hbar\omega/\mu_B H_0$ . Data for undoped sample are plotted as circles, Ta-doped are squares, and V-doped are triangles. Lines are guides for the eye.

increases gradually as the temperature is lowered below  $\sim 200$  K. At lower temperatures, both samples exhibit a rapid increase in  $\chi_{\text{ESR}}(0)$ , reaching a maximum near or below the lower CDW transition temperatures (60 K in the undoped sample, 53 K in the Ta-doped sample), before falling off at the lowest temperatures. There is no similar feature near the upper CDW transition (145 K in the undoped sample, 134 K for the Ta-doped sample). In contrast,  $\chi_{\text{ESR}}(0)$  in the V-doped sample displays a monotonic increase with decreasing temperature. It is instructive to compare the temperature dependence of  $\chi_{\text{ESR}}(0)$

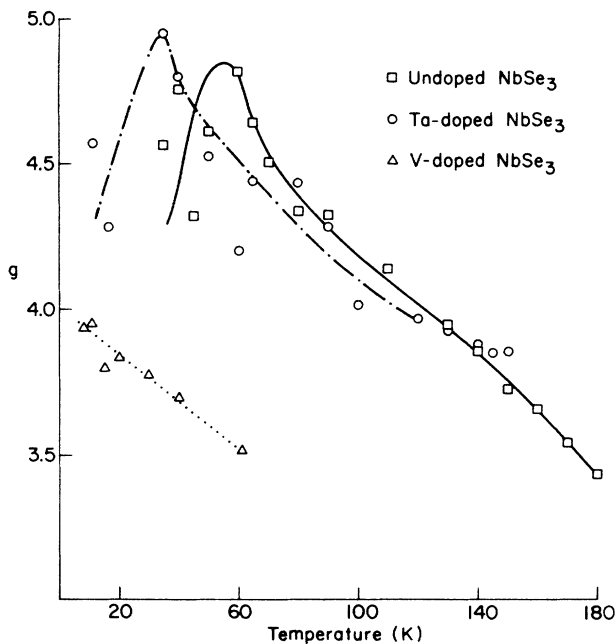


FIG. 5. Temperature dependence of the resonance linewidth. Data for the undoped sample are plotted as circles, Ta-doped are squares, and V-doped are triangles. Lines are guides for the eye.

with that of the dc susceptibility  $\chi_c$  graphed in Fig. 1. On inspection, we see that only the V-doped sample has the same qualitative temperature dependence for  $\chi_c$  and  $\chi_{\text{ESR}}(0)$ . We conclude that the resonance in the V-doped sample is due to the V moments, strongly coupled to the conduction electrons. The distinctive temperature dependence of  $\chi_{\text{ESR}}(0)$  in the undoped and Ta-doped samples argues against associating the resonance with residual magnetic impurities or defects, which would be expected to have susceptibilities which increase monotonically with decreasing temperature, as in the V-doped sample. Instead, we suggest that the resonance observed in undoped and Ta-doped  $\text{NbSe}_3$  is a conduction-electron spin resonance (CESR). Although observation of a CESR is relatively rare in metals because of fast conduction-electron relaxation times, we suggest that in  $\text{NbSe}_3$  the conductivity anisotropy limits the electronic mean free path perpendicular to the chain axis. The result is slow diffusion of the resonant moments relative to isotropic metals; this effect is reflected in the considerable asymmetry of the resonance line shape in the present experiment.

Band-structure calculations<sup>8</sup> indicate that the Fermi surface of  $\text{NbSe}_3$  has five sheets, four of which are almost completely gapped by CDW formation, and a remaining sheet which is responsible for the metallic character of  $\text{NbSe}_3$  at low temperature. The temperature dependence of  $\chi_{\text{ESR}}(0)$  can be explained by considering the effect of CDW gap formation on the electronic density of states on both the CDW and non-CDW bands. While the density of states for unpaired electrons on the CDW band drops monotonically with temperature, we have proposed elsewhere<sup>9</sup> that a peak in the density of states can result from induced gap formation on the non-CDW band as the temperature is lowered below the Peierls transition. The effect of the induced gap on the non-CDW electronic density of states at the Fermi level,  $n(E_F)$ , is demonstrated in Fig. 6 for a hypothetical metal with a CDW and non-CDW band. On the CDW band, given by the dotted line, the CDW gap opens at the Fermi level; at the same time, the non-CDW band, indicated with a solid line, develops a gap  $\Delta_i$  above the Fermi level [Fig. 6(a)]. Both the CDW and induced gaps are accompanied by a  $\sqrt{E}$  density of states anomaly at the gap edge; if  $\Delta_i$  is much further than  $k_B T$  from  $E_F$ , the anomaly will not appreciably affect  $n(E_F)$ . However, as the CDW gap develops, the edge of  $\Delta_i$  approaches  $E_F$ , leading to an increase in  $n(E_F)$  [Fig. 6(b)]. Finally, as the CDW gap saturates at its full value, the anomaly in the non-CDW band may be driven completely through the Fermi level, leading to a net reduction in  $n(E_F)$  [Fig. 6(c)]. It is likely that the peak in the inverse Hall constant observed over the same temperature range in undoped  $\text{NbSe}_3$  (Refs. 10 and 11) results from the same sequence of events. We propose that the resonance observed in the undoped and Ta-doped samples is a CESR involving unpaired electrons on the non-CDW band. The peak in the temperature dependence of the resonant moment susceptibility  $\chi_{\text{ESR}}(0)$  results from driving a density of states anomaly associated with the induced gap on this band through the Fermi lev-

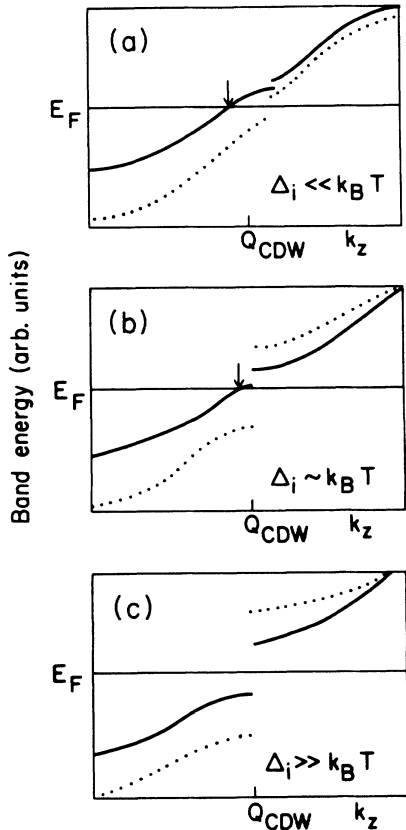


FIG. 6. Development of gaps on the CDW (dotted line) and non-CDW (solid lines) bands. As the CDW and induced gaps ( $\Delta_i$ ) grow, the density of states on the non-CDW band, indicated by the arrow, (a) increases, (b) reaches a maximum, and (c) is driven to zero as the induced gap passes through the Fermi level.

el. Since the non-CDW Fermi surface is not expected to be isotropic<sup>8</sup> and since undoped NbSe<sub>3</sub> is metallic at low temperature, we stress that the induced gap does not approach the Fermi level in all directions in the zone, so there is no complete metal-insulator transition.

Adjustment of the non-CDW band mass is expected to accompany the major modifications made to this band by induced gap formation. Thus, it is reasonable to expect that the temperature dependence of the Landé  $g$  factor, plotted in Fig. 4 for each of the samples, is the result of the same induced gap formation as previously reflected in the temperature dependence of  $\chi_{\text{ESR}}(0)$ . Like  $\chi_{\text{ESR}}(0)$ , the  $g$  factors for the undoped and Ta-doped samples increase as the temperature is lowered; a maximum is observed at the same temperature for which  $\chi_{\text{ESR}}(0)$  is a maximum. Again, as the temperature is lowered still further, the  $g$  factor drops. The  $g$  factor of the V-doped sample increases monotonically with decreasing temperature.

Although relating the  $g$  factor and the electronic mass  $m^*$  requires a full knowledge of the band structure, we estimate<sup>12</sup> that

$$\frac{m}{m^*} \sim \frac{g}{2} \quad (2)$$

by assuming there is a single resonance level and ignoring spin-orbit coupling. In the alkali metals, the  $g$  factor of the observed CESR's are very near the free-electron value  $g = 2.0023 \dots$ ; the anomalously large  $g$  factor observed in the present experiment suggests a rather low electronic mass for the non-CDW electrons in NbSe<sub>3</sub>. Shubnikov-de Haas oscillation measurements<sup>13,14</sup> on NbSe<sub>3</sub> below 4 K are dominated by a single ellipsoidal pocket of electrons with low effective mass and moderate anisotropy. The published reports, in addition to a cyclotron resonance experiment,<sup>15</sup> find that these electrons have an effective mass of  $\sim 0.25$ – $0.3 m$  along the chain and  $\sim 0.7$ – $0.8 m$  in the transverse direction.  $g$  factors in the range 2.4–3.2 were extracted from the high-field spin splitting. By extrapolating the  $g$  factors from the ESR experiment to the temperature range of the Shubnikov-de Haas and cyclotron resonance experiments, we find  $g(4.2 \text{ K}) = 4 \pm 1$ . If the complete  $g$  shift is determined by our simple band-structure considerations and not by dynamic effects, then the effective mass of the resonant electrons is in the range 0.4–0.6  $m$ , in agreement with the effective masses found in the Shubnikov-de Haas and cyclotron resonance experiments. Since the resonance in the V-doped sample is of mixed character, it is expected that the observed  $g$  factor should fall between the conduction-electron  $g$  factor found in undoped NbSe<sub>3</sub> and the V-free-ion moment, which is very close to 2.0.<sup>16</sup> However, any calculation of the  $g$  factor of this coupled system would require a more complete understanding of the nature of the V-moment-conduction-electron interaction.

Up to this point we have concentrated on the properties of the resonance which are determined by the electronic band structure. Examination of the resonance linewidth, plotted in Fig. 5, reveals that these considerations affect the spin relaxation as well. The resonance linewidth for the undoped and Ta-doped samples has qualitatively the same temperature dependence as the susceptibility  $\chi_{\text{ESR}}(0)$  and the  $g$  factor. Starting at high temperature, the Ta-doped-sample linewidth increases approximately linearly with the decrease in temperature; the linewidth then rapidly increases to a maximum near the lower transition temperature before dropping off at lower temperatures. The undoped sample linewidth is essentially temperature independent above the lower CDW transition, but increases to a maximum about 10 K below the lower transition, before falling off at the lowest temperatures. The linewidth of the V-doped sample is temperature independent within the experimental uncertainty. In our analysis of the linewidth, we will be especially interested in explaining the striking similarity in the temperature dependence of the linewidth,  $g$  shift, and resonant-moment susceptibility.

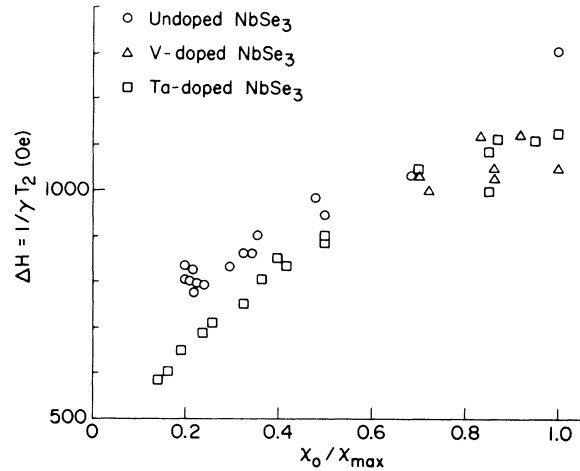
If the spin relaxation in NbSe<sub>3</sub> is governed by random dipolar field inhomogeneities in the presence of exchange narrowing, the  $g$ -shift and linewidth may be related through the static susceptibility  $\chi_1$ , the dipolar interaction strength  $\omega_D$ , and the spin-relaxation time  $\tau$ :<sup>17</sup>

$$\Delta H = \frac{\omega_D^2 \tau}{\chi_1}, \quad (3)$$

$$\frac{\Delta g}{g} = \frac{\omega_D^2 \tau^2}{2\chi_1} \quad (4)$$

Taking the maximum excess linewidth to be  $\sim 400$  Oe and  $\tau \sim 10^{-14}$  s from optical reflectance measurements,<sup>18</sup> we estimate a fractional  $g$  shift  $\Delta g/g \sim 10^{-5}$ . We conclude that the observed linewidth and shift cannot be simultaneously explained as completely dynamic effects. In fact, the anomalously large  $g$  shift observed in  $\text{NbSe}_3$  strongly suggests that the  $g$  shift is mostly intrinsic, resulting from the quasi-one-dimensional band structure of  $\text{NbSe}_3$ . Assuming that the dynamic contribution to the  $g$  shift is insignificant, the linewidth measurements can be explained in two limiting situations.

In the first, the excess linewidth results from a distribution of resonance  $g$  factors expected for the complicated and anisotropic Fermi surface of the resonant conduction



\*Present address: Physics Division, Los Alamos National Laboratory, Los Alamos, NM 87545.

- <sup>1</sup>P. Haen, P. Monceau, B. Tissier, G. Waysand, A. Meerschaut, P. Molinie, and J. Rouxel, in *Low Temperature Physics*, Proceedings of the 14th Conference on Low-Temperature Physics, Otaniemi, Finland, edited by M. Krusius and M. Vuorio (American Elsevier, New York, 1975); K. Tsutsumi, T. Takagaki, M. Yamamoto, Y. Shiozaki, M. Ido, T. Sambongi, K. Yamaya, and Y. Abe, *Phys. Rev. Lett.* **39**, 1675 (1977); R. M. Fleming, D. E. Moncton, and D. B. McWhan, *Phys. Rev. B* **18**, 5560 (1978).
- <sup>2</sup>J. D. Kulick and J. C. Scott, *Solid State Commun.* **32**, 217 (1979).
- <sup>3</sup>J. C. Lasjaunias and P. Monceau, *Solid State Commun.* **41**, 911 (1982).
- <sup>4</sup>Roald Hoffmann, Sason Shaik, J. C. Scott, Myung-Hwan Whangbo, and Mary J. Foshee, *J. Solid State Chem.* **34**, 263 (1980).
- <sup>5</sup>Neil W. Ashcroft and N. David Mermin, *Solid State Physics* (Holt, Rinehart, and Winston, Philadelphia, 1976), p. 658.
- <sup>6</sup>Freeman J. Dyson, *Phys. Rev.* **98**, 349 (1955).
- <sup>7</sup>George Feher and A. F. Kip, *Phys. Rev.* **98**, 337 (1955).
- <sup>8</sup>Nobuyuki Shima and Hiroshi Kamimura, in *Theoretical Aspects of Band Structures and Electronic Properties of Pseudo-One Dimensional Solids*, edited by Hiroshi Kamimura (Reidel, Dordrecht, 1985).
- <sup>9</sup>M. C. Aronson, M. B. Salamon, K. K. Christenson, and K. Ghiron, preceding paper, *Phys. Rev. B* **38**, 10 468 (1988).
- <sup>10</sup>N. P. Ong and J. W. Brill, *Phys. Rev. B* **18**, 5265 (1978).
- <sup>11</sup>G. X. Tessema and N. P. Ong, *Phys. Rev. B* **23**, 5607 (1981).
- <sup>12</sup>M. H. Cohen and E. I. Blount, *Philos. Mag.* **5**, 115 (1959).
- <sup>13</sup>P. Monceau, *Solid State Commun.* **24**, 331 (1977).
- <sup>14</sup>R. M. Fleming, J. A. Polo, Jr., and R. V. Coleman, *Phys. Rev. B* **17**, 1634 (1978).
- <sup>15</sup>R. J. Wagner and N. P. Ong, *Solid State Commun.* **46**, 491 (1983).
- <sup>16</sup>A. A. Abragam and B. Bleaney, in *Electron Paramagnetic Resonance of Transition Ions* (Clarendon, Oxford, 1970).
- <sup>17</sup>K. Kawasaki, *Prog. Theor. Phys.* **39**, 285 (1968).
- <sup>18</sup>H. P. Geserich, G. Scheiber, F. Levy, and P. Monceau, *Solid State Commun.* **49**, 335 (1984).
- <sup>19</sup>Y. Yafet, in *Solid State Physics*, edited by F. Seitz and D. Turnbull (Academic, New York, 1963).
- <sup>20</sup>R. Blinc and B. Zeks, in *Soft Modes in Ferroelectrics*, edited by B. Zeks (North-Holland, Amsterdam, 1974), Chap. 9.